Molecules and Cells

march5 Governs the Convergence and Extension Movement for Organization of the Telencephalon and Diencephalon in Zebrafish Embryos

Jangham Jung[1], Issac Choi[1], Hyunju Ro[1], Tae-Lin Huh[2], Joonho Choe[3], and Myungchull Rhee[1,*]

[1]Department of Life Science, BK21 Plus Program, Graduate School, Chungnam National University, Daejeon 34134, Korea, [2]School of Life Sciences and Biotechnology, College of Natural Sciences, Kyungpook National University, Daegu 41566, Korea, [3]Department of Biological Sciences, Korea Advanced Institute of Science and Technology, Daejeon 34141, Korea
*Correspondence: mrhee@cnu.ac.kr
https://doi.org/10.14348/molcells.2019.0210
www.molcells.org

MARCH5 is a RING finger E3 ligase involved in mitochondrial integrity, cellular protein homeostasis, and the regulation of mitochondrial fusion and fission. To determine the function of MARCH5 during development, we assessed transcript expression in zebrafish embryos. We found that *march5* transcripts were of maternal origin and evenly distributed at the 1-cell stage, except for the mid-blastula transition, with expression predominantly in the developing central nervous system at later stages of embryogenesis. Overexpression of *march5* impaired convergent extension movement during gastrulation, resulting in reduced patterning along the dorsoventral axis and alterations in the ventral cell types. Overexpression and knockdown of *march5* disrupted the organization of the developing telencephalon and diencephalon. Lastly, we found that the transcription of *march5* was tightly regulated by the transcriptional regulators CHOP, C/EBPα, Staf, Znf143a, and Znf76. These results demonstrate the essential role of March5 in the development of zebrafish embryos.

Keywords: convergence and extension movement, diencephalon, March5/MITOL, telencephalon, ubiquitin proteasome system

INTRODUCTION

Membrane-associated RING-CH protein 5 (MARCH5) is an E3 ubiquitin ligase located in the mitochondrial outer membrane (with the E3 ligase domain facing the cytoplasm) and is involved in a variety of mitochondrial and cellular processes (for review; Nagashima et al., 2014). For example, MARCH5 ubiquitylates the mitochondrial outer membrane proteins involved in mitochondrial fusion such as mitofusin 1 (Mfn1), which regulates mitochondrial docking and fusion, and Mfn2, which stabilizes the interactions between mitochondria. Increased expression of Mfn1 in MARCH5-depleted cells enhances mitochondrial fusion but interferes with fission (Chen et al., 2003; Park and Cho, 2012; Park et al., 2010). Ubiquitylation of Mfn2 generates a mitochondrion-associated endoplasmic reticulum membrane domain for Mfn2 oligomerization, enabling Mfn2 proteins to interact and transfer Ca^{2+} from the endoplasmic reticulum to the mitochondrion (De Brito and Scorrano, 2008; Sugiura et al., 2013; Szabadkai et al., 2006).

Another target of MARCH5, cytoplasmic dynamin-related protein 1 (Drp1), regulates mitochondrial fission. Drp1 transiently interacts with tetratricopeptide repeats in the outer-membrane-associated protein Fis1 via cytosolic adaptor proteins Mdv1 and Caf4 (Lackner et al., 2009; Mears et

Received 19 September, 2019; revised 25 November, 2019; accepted 4 December, 2019; published online 7 January, 2020

eISSN: 0219-1032

al., 2011) while MARCH5 counteracts mitochondrial fission by marking Drp1 and Fis1 for degradation (Nakamura et al., 2006; Yonashiro et al., 2006). MARCH5 also negatively regulates mitochondrial fission via stress-induced degradation of mitochondrial dynamics protein 49 kDa (MiD49) (Cherok et al., 2017; Xu et al., 2016). MiD49 is located in the mitochondrial outer membrane and recruits Drp1 to the mitochondrial surface rather than the peroxisomal surface; thus, MiD49 is thought to facilitate Drp1-directed mitochondrial fission (Palmer et al., 2011; Zhao et al., 2011).

MARCH5 marks mitophagy receptor FUN14 domain-containing protein 1 for degradation in response to hypoxia (Wu et al., 2017). MARCH5 also regulates mitochondrial transport via the degradation of abnormal proteins, such as microtubule-associated protein 1B, which interfere with dynein motor function and block the transport of mitochondria along axonal microtubules (Yonashiro et al., 2012).

Despite the many reports describing the various molecular functions of MARCH5 in mammalian cells, its embryological functions have yet to be described. Therefore, we conducted whole-mount *in situ* hybridization (WISH) and induced ectopic expression and knockdown of *march5* in zebrafish embryos to investigate the role of MARCH5 in vertebrate embryogenesis.

MATERIALS AND METHODS

Zebrafish care and embryos

Wild-type (WT) zebrafish were obtained from Korea Zebrafish Organogenesis Mutant Bank (ZOMB) and grown at 28.5°C. Embryos were obtained through natural spawning and raised, and staged as described previously (Kimmel et al., 1995; Westerfield, 2000). Embryonic pigmentation was blocked by treating the embryos with 0.002% phenylthiourea after onset of somitogenesis.

Sequence analysis

March5 sequence similarity searches to identify homologous sequences were performed as described previously (Kim et al., 2008) and phylogenic analysis of March5 was conducted at http://www.treefam.org.

Molecular cloning

Total RNA was isolated from the embryos at various stages using the easy BLUE total RNA extraction Kit (iNtRON Bio, Korea) according to the manufacturer's guidelines. cDNA was synthesized using Superscript III reverse transcriptase (Invitrogen, USA) as described in (Kumar et al., 2017). For overexpression studies, the open reading frame (ORF) of *march5* was subcloned into the pcGlobin2 vector between the restriction sites for Xho1 and EcoR1 (Ro et al., 2004).

Morpholino, *in vitro* transcription, and microinjections

Splicing-blocking morpholinos (E1/I1: 5'TTTGTTTCTTTCACTTACCTGTCCACG3') were purchased from Gene-Tools (USA), and dissolved in water. *march5*-specific morpholinos (0.8 to 1 ng) or control morpholinos were injected into zebrafish embryos at the 1-cell stage. *march5* mRNA was synthesized using the Ambion mMESSAGE mMACHINE kit according to the manufacturer's instructions. mRNAs were dissolved in nuclease-free water and diluted in 0.5% phenol red solution for microinjection via a Picopump microinjection device (World Precision Instruments, USA).

Whole-mount *in situ* hybridization (WISH)

Embryos were fixed in 4% paraformaldehyde (PFA) overnight, and dehydrated in 100% methanol. Embryos after 24 h post-fertilization (hpf) were digested with 10 μg/ml protease K (Thermo Scientific, USA). WISH was performed with minor modifications as described in (Kumar et al., 2019; Thisse et al., 1993). Antisense probes of *march5* were synthesized from a specific region within the ORF. Antisense probes of *march5* were synthesized using the DIG RNA Labeling Kit (SP6/T7) (Roche, USA).

Cell culture

HEK293T (human embryonic kidney 293T) cells were obtained from KCLB (Korean Cell Line Bank, Korea) for the Dual-Luciferases assay. HEK 293T cells were cultured in Dulbecco's modified Eagle medium (DMEM; Welgene, Korea) containing 10% fetal bovine serum (FBS; Welgene) and 1% Antibiotic-Antimycotic solution (Gibco, USA).

Luciferase activity assay

Cells were harvested and lysates were collected 24 h post transfection. Firefly and Renilla luciferase activities were measured using a Dual-Luciferase Reporter Assay System (Promega, USA) according to the manufacturer's instructions. Relative luciferase activities are the ratios of the activity of firefly luciferase to that of the Renilla luciferase control.

Reverse transcription-quantitative polymerase chain reaction (RT-qPCR)

Total RNA from WT and *march5* morpholino injected zebrafish embryos at 4.7 hpf was extracted by RNAiso Plus reagent (TaKaRa Bio, Japan), according to the manufacturer's protocol. The PrimeScript First strand cDNA synthesis kit (TaKaRa Bio) was applied for cDNA generation. qPCR was performed using SYBR-Green qPCR mix (TaKaRa Bio) in a Thermal Cycler Dice Real-Time system TP950 1 Set (TaKaRa Bio). Each assay was performed in triplicate. The specificity of the amplified products was determined by corresponding melting curve analysis. Primers used for RT-qPCR are listed in Supplementary Table S1.

Statistical analysis

All data are presented as mean ± SD. Statistically significant differences between the two groups were determined using the two-tailed Student's *t*-test. One-way ANOVA was used for comparisons among multiple groups. $P < 0.05$ was considered to indicate a statistically significant difference. Data analysis were carried out using SPSS 17.0 (IBM, USA).

RESULTS

march5 is maternally expressed and restricted to the optic vesicles, telencephalon, midbrain, and hindbrain in embryos at 18 hpf

To investigate the contribution of *march5* to vertebrate embryogenesis, we examined spatiotemporal expression in zebrafish embryos at various developmental stages. *march5* was expressed both maternally and zygotically because *march5* transcripts were detected by reverse transcriptase polymerase chain reaction (RT-PCR) at the 1-cell stage, and the expression persisted until 24 hpf. WISH confirmed that *march5* is expressed at the 1-cell stage (Fig. 1A) and revealed evenly distributed transcripts in zygotes at the sphere and shield stages (Figs. 1B and 1C). *march5* transcripts were localized to the central nervous system at 10 and 12 hpf (Figs. 1D and 1E) and restricted to the optic vesicles, telencephalon, midbrain, and hindbrain at 18 hpf (Fig. 1F). This pattern remained at 24 hpf, with *march5* transcripts restricted to the eyes, telencephalon, diencephalon, tegmentum, optic tectum, cerebellum, and rhombomeres (Figs. 1G and 1H). Thus, *march5* likely contributes to the development of these regions.

Ectopic expression and knockdown of *march5* cause developmental defects in the brain and eyes and dorsoventralization of zebrafish embryos

Microinjection of *march5* mRNA into zebrafish embryos at the 1-cell stage to induce ectopic expression resulted in notochords that were shorter along the anterior-posterior (A–P) axis but that mediolaterally expanded in comparison to those of control embryos at 24 hpf (Figs. 2A-2C). Interestingly, repression of *march5* expression in embryos at the 1-cell stage via microinjection of *march5*-specific antisense oligonucleotide morpholinos (*march5* MOs; 0.8 ng per embryo) also resulted in a shortened A–P axis as well as a reduced eye diameter (Fig. 2F) in comparison to those of 5-mismatch controls (Fig. 2E) and WT embryos at 24 hpf (Fig. 2D). We categorized the knockdown defects into three classes on the basis of their severity: class I (Fig. 2G), embryos with developmental delay but no distinguishable axial defect; class II (Fig. 2H), embryos with reduced brain volume, poor eye devel-

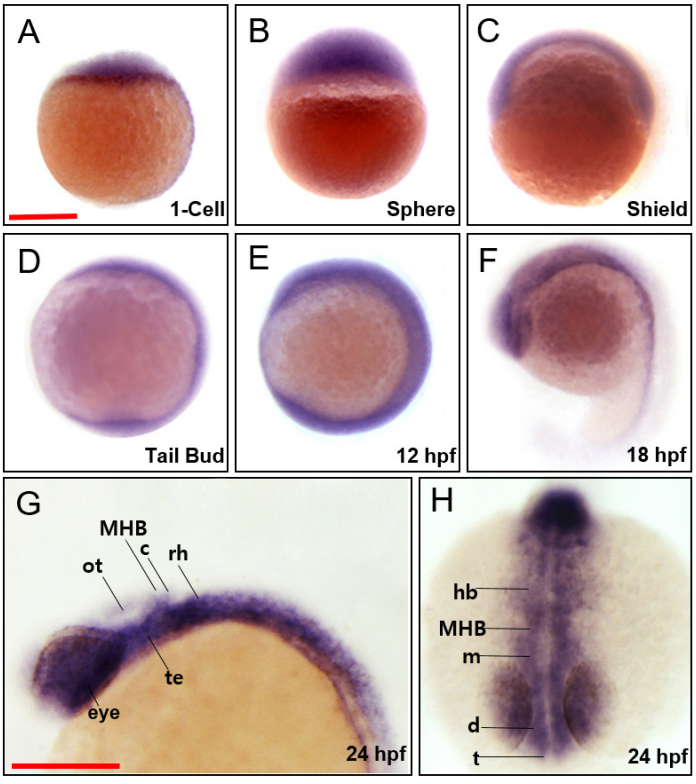

Fig. 1. Spatiotemporal expression patterns of zebrafish *march5*. WISH analysis of *march5* at 1 cell through 24 hpf. (A) *march5* was expressed in the blastodisc at 1-cell stage, indicating it is maternally expressed. (B) After MBT (512-cell), *march5* was expressed in deep cell layer (DEL) and enveloping layer (EVL) except I-YSL (yolk syncytial layer). (C) *march5* was expressed in both ventral & dorsal region at shield stage. (D-F) The transcripts were abundant in the central nervous system at 10 hpf through 18 hpf. (F) At 18 somite, *march5* transcripts were distributed in the precursor region of brain along the AP axis. (G and H) *march5* expression patterns at 24 hpf zebrafish embryo stage. Lateral (G) and anterior view (H) of the embryos labeled with *march5* antisense probe at 24 hpf. *march5* was expressed in the forebrain through the notochord including the telencephalon, diencephalon, tegmentum, optic tectum, cerebellum and rhombomere. All embryos were collected synchronously from WT zebrafish for WISH analysis at the corresponding stages. MHB, midbrain hindbrain boundary; ot, optic tectum; c, cerebellum; rh, rhombomere; te, tegmentum; hb, hindbrain; m, midbrain; d, diencephalon; t, telencephalon. (A-H) Scale bars = 250 μm.

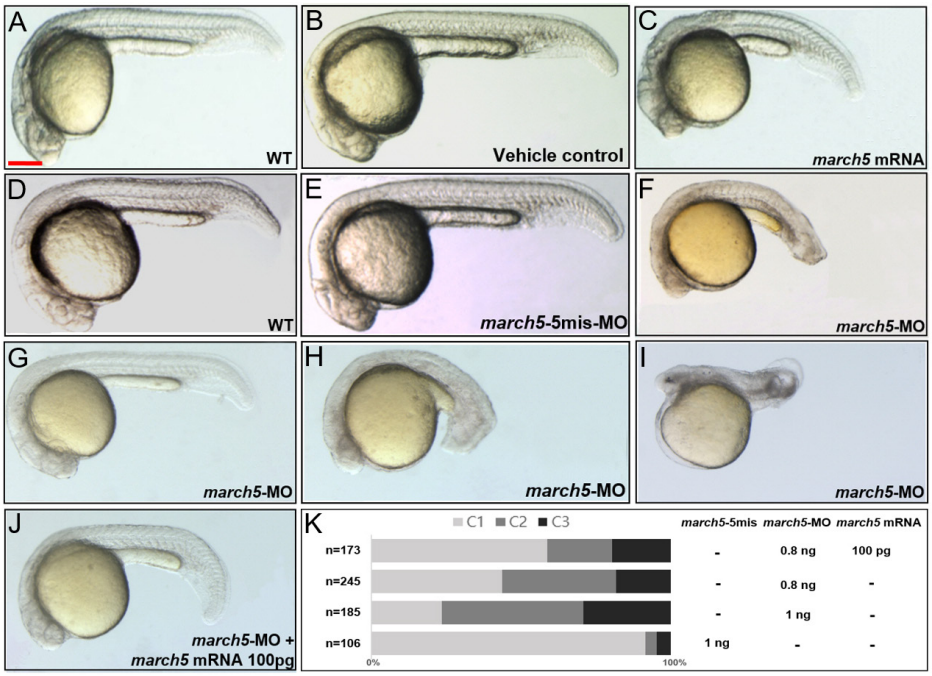

Fig. 2. Overexpression and knockdown of *march5* in zebrafish embryos. (A) WT zebrafish embryo, (B) vehicle control injected with the same volume of phenol red dye in distilled water as the volume of the mRNAs injected, and (C) *march5* mRNA injected embryo. Microinjection of *march5* mRNA (50 pg) into embryos at 1-cell stage for overexpression of *march5*. (D) WT, (E) 5-mismatch MO, and (F) *march5* MO that 0.8 ng of *march5* morpholino was injected into embryos at 1-cell stage for knockdown of *march5*. (G-J) At 24 hpf, embryos injected with *march5* MO and coinjected with *march5*-MO and *march5* mRNA. (G-I) *march5* morphants are categorized as Class 1 through 3. (J) Rescue with *march5* mRNA after injection of *march5*-MO. (K) The proportion of normal appearing embryos (C1) is increased after recue with *march5* mRNA. (A-J) Scale bars = 250 μm.

opment, and shortened body axis; class III (Fig. 2I), embryos with truncated head and no discernible axial structure. As shown in Figure 2K, *march5* MOs increased defects in class II and class III embryos in a dose-dependent manner; when the amount of *march5* MOs per embryo was increased from 0.8 to 1 ng, class I and II defects increased from 37% and 18% to 57% and 35%, respectively.

The defects in the A–P axis of the notochord induced by *march5* MOs (0.8 ng per embryo) were rescued by overexpression of *march5* (100 pg mRNA per embryo); the reduction in brain volume was partially rescued (Fig. 2J). Together, these data strongly suggest that proper expression of *march5* is critical to the development of the A–P axis, notochord, and brain.

Molecular events associated with the developmental defects induced by *march5* MOs

Cellular rearrangements that reshape the blastoderm into a characteristic vertebrate body plan begin at approximately 4 hpf. At 5 hpf, cells at the margin internalize and form the so-called hypoblast, the precursor of the mesoderm and endoderm (Solnica-Krezel, 2005). We thus examined whether an impairment of the normal gastrulation process results in morphological defects, such as a shortened A–P axis in the *march5* morphants at 24 hpf (Fig. 2H). We conducted WISH analysis of marker genes known to be critical for cell fate specification, including *gsc* and *chd* for the dorsal region, *bmp2b* for the ventral region, and *ntl* for the mesoderm (Barth et al., 1999; Fisher and Halpern, 1999; Kishimoto et al., 1997; Schulte-Merker et al., 1994). Transcript levels of the two dorsal markers, *gsc* and *chd* were remarkably reduced in the dorsal region, accompanying shrinkage of the two gene-expressing domains (Figs. 3C and 3F) in *march5* morphants at 4.7 hpf when compared with those of WT and the 5'-mismatch control (Figs. 3A, 3B, 3D, and 3E). In contrast transcripts level of the ventral marker, *bmp2b* was robustly elevated in the ventral region to cause significant expansion of *bmp2b* expressing domain (Fig. 3I) in *march5* morphants at 4.7 hpf in comparison to those of WT (Fig. 3G) and the 5'-mismatch control (Fig. 3H). Furthermore, quantitative studies of *march5* morphants at 4.7 hpf using RT-qPCR showed similar patterns to the spatiotemporal expression patterns of the two dorsal markers, *gsc* and *chd* as well as the ventral marker, *bmp2b* (Supplementary Fig. S1). These results suggest that March5 contributes to dorsalizing process in zebrafish embryos. It is thus conceivable that proper spatiotemporal expression of *march5* is essential for formation of the normal dorsoventral axis in zebrafish embryos.

march5 contributes to convergent extension (CE)

During gastrulation, CE of both ectodermal and mesendodermal cells leads to mediolateral narrowing and A–P extension of the emerging embryonic body axis (Solnica-Krezel, 2005). At the shield stage, cells deep underneath the superficial

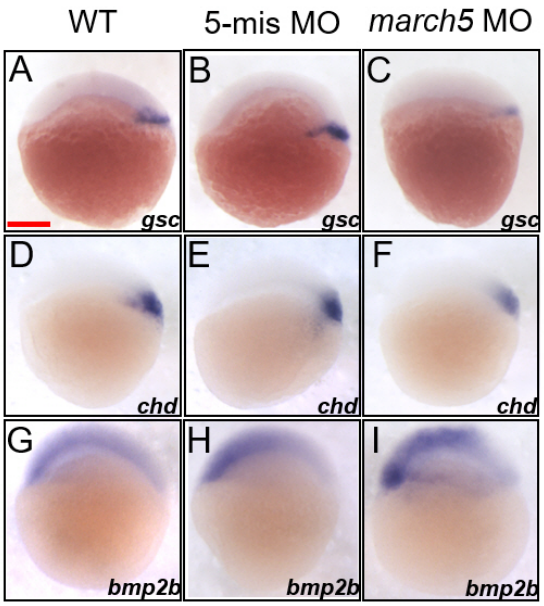

Fig. 3. Knock-down of *march5* expression alters dorso-ventral patterning at 4.7 hpf. (A-F) WISH analysis of *march5* in dorso-ventral axis development using dorsal markers, *gsc* and *chd* at 4.7 hpf. WT embryos (A and D), embryos injected with 5-mismatch as control (B and E), and *march5* MO (C and F). *march5* morphants showed narrower and reduced expression pattern for *gsc* (C) and the level of *chd* transcripts was significantly reduced in the dorsal region (D-F). (G-I) Embryos were examined for the expression of ventral marker, *bmp2b* at 4.7 hpf. Transcripts of *bmp2b* in WT (G) and 5-mis MO control (H). Injection of *march5*-MO caused notable expanded *bmp2b* expression domains, circumference around the germ ring region at 4.7 hpf (I). (A-I) Scale bars = 200 μm.

noninvoluting endocytic marginal (NEM) cell domain involute to form the nascent hypoblast of the embryonic shield, whereas cells within the NEM cell cluster form a loose mass of forerunner cells in front of the blastoderm margin (D'Amico and Cooper, 1997). To examine if MARCH5 is essential for CE, we first analyzed the expression pattern of *ntl*, a marker of mesendodermal cells in zebrafish embryos with ectopic expression or knockdown of *march5*. For ectopic expression, 50 pg *march5* mRNA was injected into embryos at the 1- to 2-cell stage. WISH for *ntl* revealed that overexpression of *march5* hindered extension of posterior paraxial mesendodermal cells, resulting in a shorter A–P axis and mediolateral expansion at 8 hpf (Fig. 4B) in comparison to that in the control (Fig. 4A). By contrast, knockdown of *march5* generated a partial axial mesendoderm, which left the posterior region separated at 8 hpf (Fig. 4D), rather than a complete axial mesoderm, as seen in the controls (Figs. 4A and 4C).

The nascent hypoblast formed during involution then moves toward the animal pole (Trinkaus, 1993), and at 60% epiboly, the dorsal forerunner cells (DFCs) develop at the leading edge of the blastoderm (D'Amico and Cooper, 1997). To examine if the defective involution of the axial hypoblast disrupts the formation of DFCs in zebrafish embryos, we studied the expression pattern of the marker gene *sox17*. At 8 hpf, *sox17* expression in control embryos revealed the migration of DFCs toward the posterior region in front of the advancing blastoderm margin (Fig. 4E). However, these DFCs were dispersed in embryos overexpressing *march5* (Fig. 4F). By contrast, knockdown of *march5* substantially reduced the area of *sox17* expression (Fig. 4H). In addition, the development of Kupffer's vesicle was severely retarded in *march5* morphants after gastrulation (data not shown). These data suggest that *march5* regulates the movement of the hypoblast to initiate DFC formation at the blastoderm margin during gastrulation in zebrafish embryos (Supplementary Fig. S2).

march5 controls patterning of the forebrain and hindbrain fields during gastrulation

We next examined the embryological consequences of *march5* overexpression and knockdown on brain development. Specifically, two-color WISH was performed at 10 and 18 hpf for *fgf8* and *krox20*, markers of the midbrain–hindbrain boundary, hindbrain, and rhombomere (Oxtoby and Jowett, 1993; Reifers et al., 1998). The analysis demonstrated that the distance between the midbrain–hindbrain boundary (marked by an asterisk in Fig. 5C) and rhombomere 3 was shortened along the A–P axis by approximately 3-fold in *march5* morphants in comparison to those of WT and 5-mismatch MO controls (Figs. 5A and 5B) at 18 hpf. These results imply that the retarded CE in *march5* morphants results in the abnormal patterning of the corresponding developing brain subdomains.

We then characterized anterior neural plate development between 10 and 24 hpf by performing WISH for *rx3* and *emx3*, markers of the telencephalon (Chuang et al., 1999; Mathers et al., 1997; Morita et al., 1995; Viktorin et al., 2009). *rx3* transcripts were substantially reduced in the presumptive anterior forebrains of *march5* morphants at 10 hpf (Fig. 5F) in comparison to those of WT and 5-mismatch MO controls (Figs. 5D and 5E). The near elimination of *emx3* at 24 hpf in the ventral forebrain of embryos with *march5* knockdown (Fig. 5I) suggests that *march5* contributes to the specification of anterior forebrain precursors during gastrulation (Supplementary Fig. S3). However, *emx3* expression was only slightly decreased in the telencephalic regions of *march5* morphants in comparison to those of WT and 5-mismatch MO controls (Figs. 5G and 5H). Altogether, these data suggest that proper *march5* expression is essential for appropriate patterning of the telencephalon.

Transcriptional factors Znf143a and Znf76 regulate *march5* expression in 293T cells

We next examined the regulatory region of *march5* for the presence of *cis*-acting elements conferring transcriptional activity. Specifically, nucleotide sequences in the zebrafish *march5* promoter located between −2917 and +296 bp of the transcriptional start site were targeted because this region contains three putative binding sites for Staf (selenocysteine tRNA gene transcription-activating factor), C/EBPα (CCAAT enhancer binding protein alpha), and CHOP (C/EBP homologous protein):C/EBPα (shown in Fig. 6A). To measure the

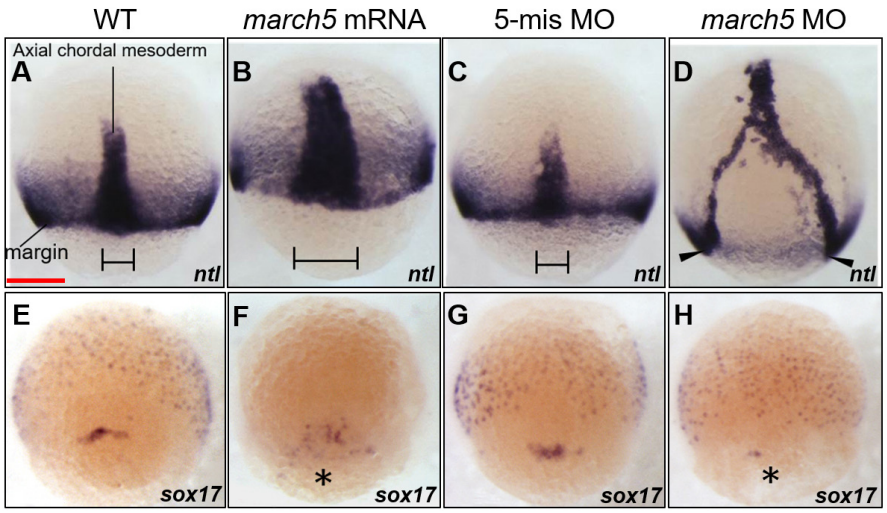

Fig. 4. Knock-down of *march5* expression causes changes in expression patterns of the molecular markers, *ntl* and *sox17* at 8 hpf. (A-D) WISH analysis using *ntl* as a molecular marker for the convergence and extension (C&E) indicates that loss of *march5* function disrupted the processes in C&E governing anterior-posterior patterning. (A) WT embryo. Microinjection of *march5* mRNA (50 pg per embryo) into wild-type embryos thickened the C&E (B). *march5* 5-mismatch control embryos had the similar expression patterns in C&E (C) to that of WT (A). In contrast, knock-down of *march5* (0.8 ng morpholino per embryo) splited the body axis (arrowheads) in *march5* morphants at 8 hpf (D). (E-H) WISH analysis with *sox17* as a molecular marker for the DFCs. *sox17* transcripts were present in the DFC of WT (E) and control embryos injected with 5-mismatch (G). Overexpression of *march5* (*march5* mRNA 50 pg per embryo) extended the area expressing *sox17* (F) while knock-down of *march5* (0.8 ng of *march5* morpholino per embryo) remarkably reduced the level of *sox17* transcripts in the DFC (asterisk) of the morphants (H). (A-H) Scale bars = 200 μm.

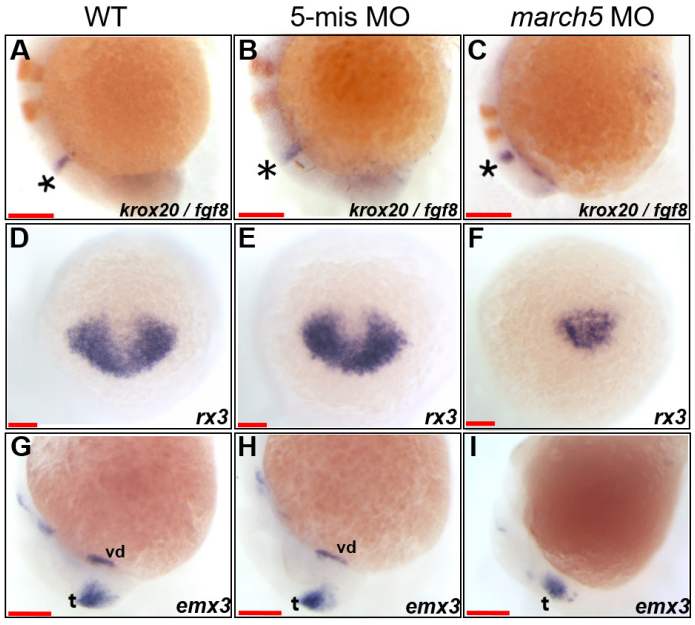

Fig. 5. *march5* knock-down reduced expression of *rx3* and *emx3* in zebrafish embryos. (A-C) Two color WISH analysis with *krox20*- and *fgf8*-specific probes detected changes in their transcripts in the MHB (asterisks) and the hindbrain, the rhombomeres (r) 3 and 5 at 18 hpf. (A) WT embryo, (B) 5-mismatch MO control, and (C) *march5* MO (0.8 ng of *march5* morpholino per embryo). (D-I) WISH analysis of *march5* MO (0.8 ng of *march5* morpholino per embryo) using *rx3* and *emx1* as probes. (D) *rx3* transcripts in the presumptive eye field and hypothalamus of WT embryos at 10 hpf. (E) Embryos injected with 5-mismatch showed similar patterns to those of WT embryos. (F) *march5* MO shows remarkable reduction of *rx3* transcripts in the presumptive eye field and hypothalamus, which abut the telencephalic primordium at 10 hpf. Transcripts of *emx3* in WT (G), 5-mismatch control (H), and *march5* MO (I) at 24 hpf. *emx3* transcripts were present in the telencephalon and ventral diencephalon in WT and 5-mismatch control whereas the ventral diencephalon expression was lost in the corresponding areas of *march5* MO. vd, ventral diencephalon; t, telencephalon. (A-I) Scale bars = 100 μm.

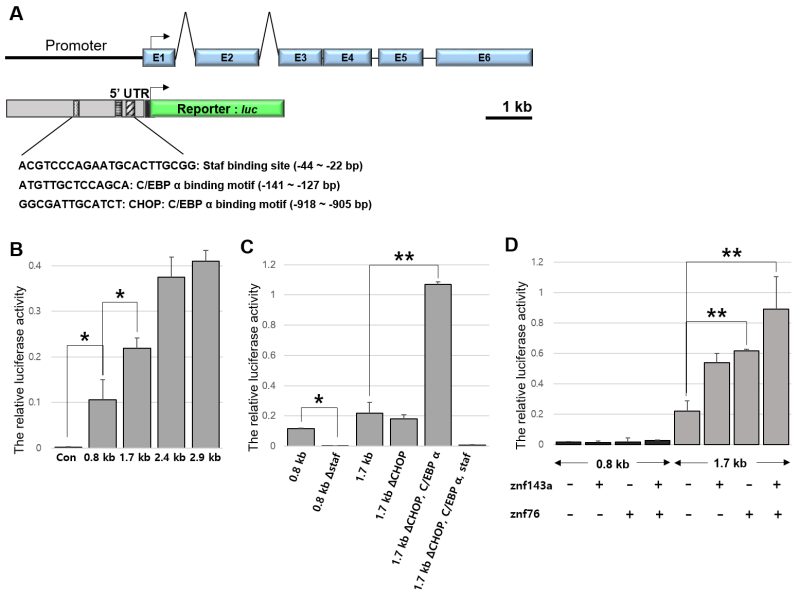

Fig. 6. Znf143a and Znf76 modulate *march5* expression. (A) Schematic representation of zebrafish *march5* genomic region and reporter construct. Six exons (EX1 to EX6) and five introns are depicted; the translation initiation site is indicated with an arrow. The firefly luciferase (*luc*) coding region was fused with the zebrafish *march5* promoter (-2904 to +296 bp). (B-D) Luciferase activity under the control of the *march5* regulatory regions. (B) Luciferase activity of a transiently transfected *march5-luc* reporter in 293T cells (**P* < 0.05 vs Con, as determined by Student's *t*-test). (C) Deletion analysis of the zebrafish *march5* promoter. Cells were transfected with the Staf, CHOP and CHOP:C/EBPα-deletion promoter-luciferase reporter plasmids. A significant difference between 1.7 kb and 1.7 kbΔCHOP, C/EBPα (***P* < 0.01, as determined by Student's *t*-test). (D) Effects of Znf143a and Znf76 proteins on the zebrafish *march5* promoter activation. Cells were co-transfected with Znf143a and Znf76 expression plasmid (empty pc2+ expression plasmid as control), and Pgl3 promoter-luciferase reporter plasmids fused with the zebrafish *march5* promoter (0.8 kb and 1.7 kb). Luciferase activity of *march5* promoter in 293T cells is expressed as normalized luciferase activity (to *Renilla* luciferase activity) relative to empty Pgl3-Basic plasmid (**P* < 0.05, ***P* < 0.01 vs 1.7kb, as determined by Student's *t*-test).

transcriptional activities of these three *cis*-acting elements, we generated four *march5-luc* reporter constructs lacking the binding sites for Staf, C/EBPα, and/or CHOP:C/EBPα (Fig. 6A), and expressed them in human embryonic kidney cells (HEK 293T cells). Transcriptional activities of the three reporter constructs containing 1.7 kb, 2.4 kb, or 2.9 kb regions were 2-, 3.5-, 4-fold higher that of the reporter containing the 0.8 kb region (Fig. 6B). The reporter construct containing the 1.7 kb region was chosen because it contains most of the *cis*- and *trans*-acting elements, such as Staf, CHOP, and C/EBPα.

To determine if CHOP and C/EBPα transcriptionally regulate *march5*, we measured the luciferase activities of the constructs with or without CHOP and/or C/EBPα in the 1.7 kb-long region. As shown in Figure 6C, deletion of the binding site for CHOP did not alter the transcriptional activity of the 1.7 kb-long region, whereas deletion of the binding sites for both CHOP and C/EBPα dramatically increased the luciferase activity by more than 5-fold relative to that of the control reporter construct containing both elements. However, deletion of the Staf binding site in addition to the CHOP:C/EBPα sites abolished transcriptional activity, observed as a complete loss of luciferase activity. Taken together, these results demonstrate that Staf functions as a potent transcriptional activator and that CHOP and C/EBPα act as transcriptional repressors of *march5*. Expression of these three transcriptional regulators may thus coordinate transcription of *march5* in zebrafish embryos.

There is notable homology between Staf and the human proteins ZNF76 and ZNF143 (Jung et al., 2019; Ragoussis et al., 1992; Tommerup and Vissing, 1995), which both contain domains similar to the Staf transactivation domains that stimulate transcription from RNA polymerase II (PolII) and PolIII small nuclear RNA (snRNA)-type promoters as well as PolII TATA box-containing mRNA promoters (Myslinski et al., 1998; Schaub et al., 1997). The high degree of sequence conservation between the zinc finger regions in *znf76* and *znf143* in the zebrafish indicate that both proteins may recognize the same Staf motif within the *march5* promoter. Luciferase activity from HEK 293T cells co-transfected with plasmids harboring the *march5* promoter and those encoding Znf143a or Znf76 was increased 3-fold, and luciferase activity was increased 4-fold when cells expressed the *march5* promoter and both Znf143a and Znf76 (Fig. 6D). Thus, we postulate that *march5* is transcriptionally regulated in a finely tuned manner by CHOP, C/EBPα, Staf, Znf143a, and Znf76.

DISCUSSION

MARCH5 is a mitochondrial ubiquitin ligase that regulates mitochondrial integrity and cellular protein homeostasis via the ubiquitin proteasome system (Nagashima et al., 2014).

We demonstrate here that March5 also regulates vertebrate embryogenesis because either knockdown or ectopic expression of *march5* in zebrafish embryos retarded CE at 8 hpf, resulting in defective development of the ventral diencephalon, midbrain, and midbrain–hindbrain boundary at 24 hpf.

Beginning at 4.3 hpf, cells intercalate radially, contributing to epiboly, while cells at the margins migrate toward the animal pole to form the hypoblast. The various progenitor territories at 6 hpf are not sharply demarcated in the fate maps of zebrafish embryos (Kimmel et al., 1990; Sepich et al., 2005). We thus examined the expression of morphogenetic markers at pre-gastrulation and gastrulation stages. We found that at 4.7 hpf, knockdown of *march5* reduced the expression of the dorsal markers but increased the expression of the ventral markers. In zebrafish, the fates of dorsal cells at the shield were once thought to be regulated by inducers expressed by the organizer; however, it is now known that the organizer represses factors secreted from ventral regions of the embryos (Niehrs, 2004), such as bone morphogenetic protein (BMP), Wnt, and Nodal family proteins; For example, ventrally expressed Wnt8 restricts the size of the zebrafish organizer in the late blastula/early gastrula by regulating the expression of the transcriptional repressors Vox and Vent, whereas during late gastrulation, the expression of these genes is maintained by BMP signaling (Ramel and Lekven, 2004; Ramel et al., 2005). In the absence of secreted BMP antagonists, Gsc has *chd*-independent functions in dorsoventral patterning and elicits complete secondary axes (Fox and Bruce, 2009). We also found that *march5* knockdown not only changed level of *wnt8* transcripts (Supplementary Fig. S4) but also reduced the transcript levels of *gsc* and *chd* (Figs. 3C and 3F).

We demonstrated that *march5* was transcriptionally regulated at CHOP and C/EBP binding sites. CHOP is a developmentally regulated nuclear protein that inhibits *wnt8*-mediated dorsal development in *Xenopus* embryos (Horndasch et al., 2006). However, CHOP also dimerizes with C/EBP via its leucine zipper domain to function as a dominant negative inhibitor of gene transcription (Ron and Habener, 1992), arresting growth and inducing apoptosis under conditions of endoplasmic reticulum stress or DNA damage (Maytin et al., 2001; Talukder et al., 2002; Ubeda et al., 1996; Wang et al., 1996; Zinszner et al., 1998). Thus, CHOP and C/EBPα may work similarly to represses *march5* transcription. By contrast, we found that the binding of Znf76 and Znf143 to the Staf site in the proximal promoter of *march5* may induce transcription. Staf, a transcriptional activator originally identified in *Xenopus laevis*, enhances the transcription of snRNA and snRNA-type genes via Pol II and Pol III (Myslinski et al., 1992; Schuster et al., 1995). The Staf binding site may be a regulator of organ-specific transcription because transgenic mice expressing a *Trsp* (selenocysteine tRNA gene) transgene lacking the Staf binding site had an ~80% reduction in the levels of Sec tRNA in the brain and muscle but unaltered or elevated levels in other tissues (Carlson et al., 2009). We found that *march5* transcription in zebrafish embryos was regulated by Znf76 and Znf143, which bind with similar affinities to Staf responsive elements (Myslinski et al., 1998). It is thus most probable that Znf76 and Znf143, together with C/EBPα and CHOP, modulate *march5* transcription to regulate biological processes such as vertebrate embryogenesis.

The data presented here provide insight into the functions of a mitochondrial ubiquitin ligase during vertebrate embryogenesis. We found that expression of *march5* must be tightly regulated for proper gastrulation and CE in zebrafish embryos. Our data indicate that Znf76 and Znf143 bind to the Staf region in the *march5* promoter and modulate C/EBPα:CHOP regulation of *march5* transcription. This is the first report to show that March5 affects the functional connection between convergence and extension processes during gastrulation. The newly identified cis- and trans-regulatory elements provide new insights into the molecular mechanisms of *march5* specific transcriptional networks in zebrafish.

Note: Supplementary information is available on the Molecules and Cells website (www.molcells.org).

Disclosure

The authors have no potential conflicts of interest to disclose.

ACKNOWLEDGMENTS

This work was supported by research fund of Chungnam National University.

ORCID

Jangham Jung https://orcid.org/0000-0003-2806-3698
Issac Choi https://orcid.org/0000-0001-8228-6994
Hyunju Ro https://orcid.org/0000-0002-0829-9639
Tae-Lin Huh https://orcid.org/0000-0002-2549-7522
Joonho Choe https://orcid.org/0000-0002-8590-6666
Myungchull Rhee https://orcid.org/0000-0002-4595-7573

REFERENCES

Barth, K.A., Kishimoto, Y., Rohr, K.B., Seydler, C., Schulte-Merker, S., and Wilson, S.W. (1999). Bmp activity establishes a gradient of positional information throughout the entire neural plate. Development *126*, 4977-4987.

Carlson, B.A., Schweizer, U., Perella, C., Shrimali, R.K., Feigenbaum, L., Shen, L., Speransky, S., Floss, T., Jeong, S.J., and Watts, J. (2009). The selenocysteine tRNA STAF-binding region is essential for adequate selenocysteine tRNA status, selenoprotein expression and early age survival of mice. Biochem. J. *418*, 61-71.

Chen, H., Detmer, S.A., Ewald, A.J., Griffin, E.E., Fraser, S.E., and Chan, D.C. (2003). Mitofusins Mfn1 and Mfn2 coordinately regulate mitochondrial fusion and are essential for embryonic development. J. Cell Biol. *160*, 189-200.

Cherok, E., Xu, S., Li, S., Das, S., Meltzer, W.A., Zalzman, M., Wang, C., and Karbowski, M. (2017). Novel regulatory roles of Mff and Drp1 in E3 ubiquitin ligase MARCH5–dependent degradation of MiD49 and Mcl1 and control of mitochondrial dynamics. Mol. Biol. Cell *28*, 396-410.

Chuang, J.C., Mathers, P.H., and Raymond, P.A. (1999). Expression of three Rx homeobox genes in embryonic and adult zebrafish. Mech. Dev. *84*, 195-198.

D'Amico, L.A. and Cooper, M.S. (1997). Spatially distinct domains of cell behavior in the zebrafish organizer region. Biochem. Cell Biol. *75*, 563-577.

De Brito, O.M. and Scorrano, L. (2008). Mitofusin 2 tethers endoplasmic reticulum to mitochondria. Nature *456*, 605-610.

Fisher, S. and Halpern, M.E. (1999). Patterning the zebrafish axial skeleton

requires early chordin function. Nat. Genet. *23*, 442-446.

Fox, M.D. and Bruce, A.E. (2009). Short-and long-range functions of Goosecoid in zebrafish axis formation are independent of Chordin, Noggin 1 and Follistatin-like 1b. Development *136*, 1675-1685.

Horndasch, M., Lienkamp, S., Springer, E., Schmitt, A., Pavenstädt, H., Walz, G., and Gloy, J. (2006). The C/EBP homologous protein CHOP (GADD153) is an inhibitor of Wnt/TCF signals. Oncogene *25*, 3397-3407.

Jung, J., Udhaya Kumar, S., Choi, I., Huh, T.L., and Rhee, M. (2019). Znf76 is associated with development of the eyes, midbrain, MHB, and hindbrain in zebrafish embryos. Anim. Cells Syst. *23*, 26-31.

Kim, E.J., Ro, H., Huh, T.L., Lee, C.J., Choi, J., and Rhee, M. (2008). A novel Kinesin-like protein, Surhe is associated with dorsalization in the zebrafish embryos. Anim. Cells Syst. *12*, 219-230.

Kimmel, C.B., Ballard, W.W., Kimmel, S.R., Ullmann, B., and Schilling, T.F. (1995). Stages of embryonic development of the zebrafish. Dev. Dyn. *203*, 253-310.

Kimmel, C.B., Warga, R.M., and Schilling, T.F. (1990). Origin and organization of the zebrafish fate map. Development *108*, 581-594.

Kishimoto, Y., Lee, K.H., Zon, L., Hammerschmidt, M., and Schulte-Merker, S. (1997). The molecular nature of zebrafish swirl: BMP2 function is essential during early dorsoventral patterning. Development *124*, 4457-4466.

Kumar, A., Anuppalle, M., Maddirevula, S., Huh, T.L., Choe, J., and Rhee, M. (2019). Peli1b governs the brain patterning via ERK signaling pathways in zebrafish embryos. Gene *694*, 1-6.

Kumar, A., Huh, T.L., Choe, J., and Rhee, M. (2017). Rnf152 is essential for NeuroD expression and Delta-notch signaling in the zebrafish embryos. Mol. Cells *40*, 945.

Lackner, L.L., Horner, J.S., and Nunnari, J. (2009). Mechanistic analysis of a dynamin effector. Science *325*, 874-877.

Mathers, P., Grinberg, A., Mahon, K., and Jamrich, M. (1997). The Rx homeobox gene is essential for vertebrate eye development. Nature *387*, 603-607.

Maytin, E.V., Ubeda, M., Lin, J.C., and Habener, J.F. (2001). Stress-inducible transcription factor CHOP/gadd153 induces apoptosis in mammalian cells via p38 kinase-dependent and-independent mechanisms. Exp. Cell Res. *267*, 193-204.

Mears, J.A., Lackner, L.L., Fang, S., Ingerman, E., Nunnari, J., and Hinshaw, J.E. (2011). Conformational changes in Dnm1 support a contractile mechanism for mitochondrial fission. Nat. Struct. Mol. Biol. *18*, 20-26.

Morita, T., Nitta, H., Kiyama, Y., Mori, H., and Mishina, M. (1995). Differential expression of two zebrafish emx homeoprotein mRNAs in the developing brain. Neurosci. Lett. *198*, 131-134.

Myslinski, E., Krol, A., and Carbon, P. (1992). Optimal tRNA (Ser) Sec gene activity requires an upstream SPH motif. Nucleic Acids Res. *20*, 203-209.

Myslinski, E., Krol, A., and Carbon, P. (1998). ZNF76 and ZNF143 are two human homologs of the transcriptional activator Staf. J. Biol. Chem. *273*, 21998-22006.

Nagashima, S., Tokuyama, T., Yonashiro, R., Inatome, R., and Yanagi, S. (2014). Roles of mitochondrial ubiquitin ligase MITOL/MARCH5 in mitochondrial dynamics and diseases. J. Biochem. *155*, 273-279.

Nakamura, N., Kimura, Y., Tokuda, M., Honda, S., and Hirose, S. (2006). MARCH-V is a novel mitofusin 2-and Drp1-binding protein able to change mitochondrial morphology. EMBO Rep. *7*, 1019-1022.

Niehrs, C. (2004). Regionally specific induction by the Spemann–Mangold organizer. Nat. Rev. Genet. *5*, 425-434.

Oxtoby, E. and Jowett, T. (1993). Cloning of the zebrafish krox-20 gene (krx-20) and its expression during hindbrain development. Nucleic Acids Res. *21*, 1087-1095.

Palmer, C.S., Osellame, L.D., Laine, D., Koutsopoulos, O.S., Frazier, A.E., and Ryan, M.T. (2011). MiD49 and MiD*51*, new components of the mitochondrial fission machinery. EMBO Rep. *12*, 565-573.

Park, Y.Y. and Cho, H. (2012). Mitofusin 1 is degraded at G2/M phase through ubiquitylation by MARCH5. Cell Div. *7*, 25.

Park, Y.Y., Lee, S., Karbowski, M., Neutzner, A., Youle, R.J., and Cho, H. (2010). Loss of MARCH5 mitochondrial E3 ubiquitin ligase induces cellular senescence through dynamin-related protein 1 and mitofusin 1. J. Cell Sci. *123*, 619-626.

Ragoussis, J., Senger, G., Mockridge, I., Sanseau, P., Ruddy, S., Dudley, K., Sheer, D., and Trowsdale, J. (1992). A testis-expressed Zn finger gene (ZNF76) in human 6p21. 3 centromeric to the MHC is closely linked to the human homolog of the t-complex gene tcp-11. Genomics *14*, 673-679.

Ramel, M.C., Buckles, G.R., Baker, K.D., and Lekven, A.C. (2005). WNT8 and BMP2B co-regulate non-axial mesoderm patterning during zebrafish gastrulation. Dev. Biol. *287*, 237-248.

Ramel, M.C. and Lekven, A.C. (2004). Repression of the vertebrate organizer by Wnt8 is mediated by Vent and Vox. Development *131*, 3991-4000.

Reifers, F., Bohli, H., Walsh, E.C., Crossley, P.H., Stainier, D., and Brand, M. (1998). Fgf8 is mutated in zebrafish acerebellar (ace) mutants and is required for maintenance of midbrain-hindbrain boundary development and somitogenesis. Development *125*, 2381-2395.

Ro, H., Soun, K., Kim, E.J., and Rhee, M. (2004). Novel vector systems optimized for injecting in vitro-synthesized mRNA into zebrafish embryos. Mol. Cells *17*, 373-376.

Ron, D. and Habener, J.F. (1992). CHOP, a novel developmentally regulated nuclear protein that dimerizes with transcription factors C/EBP and LAP and functions as a dominant-negative inhibitor of gene transcription. Genes Dev. *6*, 439-453.

Schaub, M., Myslinski, E., Schuster, C., Krol, A., and Carbon, P. (1997). Staf, a promiscuous activator for enhanced transcription by RNA polymerases II and III. EMBO J. *16*, 173-181.

Schulte-Merker, S., Hammerschmidt, M., Beuchle, D., Cho, K., De Robertis, E., and Nusslein-Volhard, C. (1994). Expression of zebrafish goosecoid and no tail gene products in wild-type and mutant no tail embryos. Development *120*, 843-852.

Schuster, C., Myslinski, E., Krol, A., and Carbon, P. (1995). Staf, a novel zinc finger protein that activates the RNA polymerase III promoter of the selenocysteine tRNA gene. EMBO J. *14*, 3777-3787.

Sepich, D.S., Calmelet, C., Kiskowski, M., and Solnica-Krezel, L. (2005). Initiation of convergence and extension movements of lateral mesoderm during zebrafish gastrulation. Dev. Dyn. *234*, 279-292.

Solnica-Krezel, L. (2005). Conserved patterns of cell movements during vertebrate gastrulation. Curr. Biol. *15*, R213-R228.

Sugiura, A., Nagashima, S., Tokuyama, T., Amo, T., Matsuki, Y., Ishido, S., Kudo, Y., McBride, H.M., Fukuda, T., and Matsushita, N. (2013). MITOL regulates endoplasmic reticulum-mitochondria contacts via Mitofusin2. Mol. Cell *51*, 20-34.

Szabadkai, G., Bianchi, K., Várnai, P., De Stefani, D., Wieckowski, M.R., Cavagna, D., Nagy, A.I., Balla, T., and Rizzuto, R. (2006). Chaperone-mediated coupling of endoplasmic reticulum and mitochondrial Ca2+ channels. J. Cell Biol. *175*, 901-911.

Talukder, A.H., Wang, R.A., and Kumar, R. (2002). Expression and transactivating functions of the bZIP transcription factor GADD153 in mammary epithelial cells. Oncogene *21*, 4289-4300.

Thisse, C., Thisse, B., Schilling, T., and Postlethwait, J. (1993). Structure of the zebrafish snail1 gene and its expression in wild-type, spadetail and no tail mutant embryos. Development *119*, 1203-1215.

Tommerup, N. and Vissing, H. (1995). Isolation and fine mapping of 16 novel human zinc finger-encoding cDNAs identify putative candidate genes for developmental and malignant disorders. Genomics *27*, 259-

264.

Trinkaus, J. (1993). The yolk syncytial layer of Fundulus: its origin and history and its significance for early embryogenesis. J. Exp. Zool. *265*, 258-284.

Ubeda, M., Wang, X.Z., Zinszner, H., Wu, I., Habener, J.F., and Ron, D. (1996). Stress-induced binding of the transcriptional factor CHOP to a novel DNA control element. Mol. Cell. Biol. *16*, 1479-1489.

Viktorin, G., Chiuchitu, C., Rissler, M., Varga, Z.M., and Westerfield, M. (2009). Emx3 is required for the differentiation of dorsal telencephalic neurons. Dev. Dyn. *238*, 1984-1998.

Wang, X.Z., Lawson, B., Brewer, J.W., Zinszner, H., Sanjay, A., Mi, L.J., Boorstein, R., Kreibich, G., Hendershot, L.M., and Ron, D. (1996). Signals from the stressed endoplasmic reticulum induce C/EBP-homologous protein (CHOP/GADD153). Mol. Cell. Biol. *16*, 4273-4280.

Westerfield, M. (2000). The zebrafish book: a guide for the laboratory use of zebrafish. http://zfin.org/zf_info/zfbook/zfbk.html.

Wu, X., Wu, F.H., Wu, Q., Zhang, S., Chen, S., and Sima, M. (2017). Phylogenetic and molecular evolutionary analysis of Mitophagy receptors under hypoxic conditions. Front. Physiol. *8*, 539.

Xu, S., Cherok, E., Das, S., Li, S., Roelofs, B.A., Ge, S.X., Polster, B.M., Boyman, L., Lederer, W.J., and Wang, C. (2016). Mitochondrial E3 ubiquitin ligase MARCH5 controls mitochondrial fission and cell sensitivity to stress-induced apoptosis through regulation of MiD49 protein. Mol. Biol. Cell *27*, 349-359.

Yonashiro, R., Ishido, S., Kyo, S., Fukuda, T., Goto, E., Matsuki, Y., Ohmura-Hoshino, M., Sada, K., Hotta, H., and Yamamura, H. (2006). A novel mitochondrial ubiquitin ligase plays a critical role in mitochondrial dynamics. EMBO J. *25*, 3618-3626.

Yonashiro, R., Kimijima, Y., Shimura, T., Kawaguchi, K., Fukuda, T., Inatome, R., and Yanagi, S. (2012). Mitochondrial ubiquitin ligase MITOL blocks S-nitrosylated MAP1B-light chain 1-mediated mitochondrial dysfunction and neuronal cell death. Proc. Natl. Acad. Sci. U. S. A. *109*, 2382-2387.

Zhao, J., Liu, T., Jin, S., Wang, X., Qu, M., Uhlén, P., Tomilin, N., Shupliakov, O., Lendahl, U., and Nistér, M. (2011). Human MIEF1 recruits Drp1 to mitochondrial outer membranes and promotes mitochondrial fusion rather than fission. EMBO J. *30*, 2762-2778.

Zinszner, H., Kuroda, M., Wang, X., Batchvarova, N., Lightfoot, R.T., Remotti, H., Stevens, J.L., and Ron, D. (1998). CHOP is implicated in programmed cell death in response to impaired function of the endoplasmic reticulum. Genes Dev. *12*, 982-995.